



# Effect of the 2022 summer drought across forest types in Europe

Mana Gharun<sup>1</sup>, Ankit Shekhar<sup>2,3</sup>, Jingfeng Xiao<sup>4</sup>, Xing Li<sup>5</sup>, and Nina Buchmann<sup>2</sup>

<sup>1</sup>Department of Geosciences, Institute of Landscape Ecology, University of Münster, Münster, Germany

<sup>2</sup>Department of Environmental Systems Science, Institute of Agricultural Sciences, ETH Zürich, Zurich, Switzerland

<sup>3</sup>Agricultural and Food Engineering Department, Indian Institute of Technology Kharagpur, Kharagpur, India

<sup>4</sup>Earth Systems Research Center, University of New Hampshire, Durham, New Hampshire, USA

<sup>5</sup>School of Geography and Planning, Sun Yat-sen University, Guangzhou, China

**Correspondence:** Mana Gharun (mana.gharun@uni-muenster.de)

Received: 13 February 2024 – Discussion started: 26 February 2024

Revised: 6 August 2024 – Accepted: 4 October 2024 – Published: 11 December 2024

**Abstract.** Forests in Europe experienced record-breaking dry conditions during the summer of 2022. The direction in which various forest types respond to climate extremes during their growing season is contingent upon an array of internal and external factors. These factors include the extent and severity of the extreme conditions and the tree eco-physiological characteristics adapted to environmental cues, which exhibit significant regional variations. In this study, we aimed to (1) quantify the extent and severity of the extreme soil and atmospheric dryness in 2022 in comparison to the two most extreme years in the past (2003 and 2018), (2) quantify the response of different forest types to atmospheric and soil dryness in terms of canopy browning and photosynthesis, and (3) relate the functional characteristics of the forests to the emerging responses observed remotely at the canopy level. For this purpose, we used spatial meteorological datasets between 2000 and 2022 to identify conditions with extreme soil and atmospheric dryness. We used the near-infrared reflectance of vegetation ( $\text{NIR}_v$ ), derived from the Moderate Resolution Imaging Spectroradiometer (MODIS), and the global OCO-2 solar-induced fluorescence (GOSIF) as an observational proxy for ecosystem gross productivity to quantify the response of forests at the canopy level.

In summer 2022, southern regions of Europe experienced exceptionally pronounced atmospheric and soil dryness. These extreme conditions resulted in a 30 % more widespread decline in GOSIF across forests compared to the drought of 2018 and 60 % more widespread decline compared to the drought of 2003. Although the atmospheric and soil drought scores were more extensive and severe (indicated by a larger observed maximum  $z$  score) in 2018 com-

pared to 2022, the negative impact on forests, as indicated by declined GOSIF, was significantly larger in 2022. Different forest types were affected to varying degrees by the extreme conditions in 2022. Deciduous broadleaf forests were the most negatively impacted due to the extent and severity of the drought within their distribution range. In contrast, areas dominated by evergreen needleleaf forest (ENF) in northern Europe experienced a positive soil moisture (SM) anomaly and minimal negative vapour pressure deficit (VPD) in 2022. These conditions led to enhanced canopy greening and stronger solar-induced fluorescence (SIF) signals, benefiting from the warming. The higher degree of canopy damage in 2022, despite less extreme conditions, highlights the evident vulnerability of European forests to future droughts.

## 1 Introduction

The frequency and intensity of drought events have been rising globally, and future global warming is expected to further increase their occurrence (Seneviratne et al., 2021; Röthlisberger and Papritz, 2023). Particularly over the past 2 decades, many regions in Europe have experienced widespread drought conditions, notably during the summers of 2003, 2010, and 2018 (Bastos et al., 2020; Zhou et al., 2023). The extreme conditions caused widespread ecological disturbances (Müller and Bahn 2022) and reduced the capacity of forests for carbon uptake, thereby diminishing their potential for mitigating climate change (van der Woude et al., 2023). Additionally, heat waves and prolonged droughts

stress vegetation, making it more susceptible to other biotic and abiotic stress factors. This increased vulnerability leads to higher tree mortality, elevated wildfire risks, and a loss of biodiversity among plants and animals living at the edge of their temperature tolerance. These conditions also alter phenology and plant development, causing cascading effects on ecosystem functioning (Seidl et al., 2017).

The spatial extent and severity of drought events vary, and their impacts depend on local ecological characteristics of the forests, species-specific temperature and moisture thresholds that limit tree functioning, and adaptation strategies and acclimation of trees to more frequent and intense extreme conditions (Gessler et al., 2020). For example, comparing the extreme years of 2003 and 2018, the year 2018 was characterized by a climatic dipole, featuring extremely hot and dry weather conditions north of the Alps but comparably cool and moist conditions across large parts of the Mediterranean. Negative drought impacts appeared to affect an area that was 1.5 times larger and appeared to be significantly stronger in the summer of 2018 compared to the summer of 2003 (Buras et al., 2020).

In 2022, Europe faced its second hottest and driest year on record, with the summer of that year being the warmest summer ever recorded. Conditions in summer 2022 led to record-breaking heat-wave and drought events across many regions (Copernicus Climate Change Service, 2023). Compound drought and heat-wave conditions in 2022 caused widespread crop damage, water shortages, and wildfires across Europe. The hardest-hit areas were the Iberian Peninsula, France, and Italy, where temperatures exceeded 2.5 °C above normal, and severe droughts persisted from May to August (Tripathy and Mishra, 2023). The reduced soil moisture due to precipitation deficits and high temperatures contributed to the persistence and severity of drought, creating a positive feedback loop where dry soils led to even drier conditions (Tripathy and Mishra, 2023).

Drought and heat waves have a range of detrimental effects on trees and forests. The most immediate impact is that elevated air temperatures and increased dryness, whether in the soil or in the atmosphere, disrupt mesophyll and stomatal conductance, thereby impairing carbon uptake (Marchin et al., 2022). Plants reduce stomatal conductance under severe drought to reduce water stress at the expense of reduced rates of photosynthesis (Oren et al., 1999). Drought also increases the chance of hydraulic failure, which can lead to tree mortality (Choat et al., 2018). Additionally, rising temperatures reduce the enzymatic activity in trees, which in turn diminishes the forest's gross primary productivity (Gourlez de la Motte et al., 2020). Elevated temperatures can also increase respiration rates in both soil and trees, which reduces the forest's net carbon uptake and its ability to mitigate anthropogenic CO<sub>2</sub> emissions (van der Molen et al., 2011; Anjileli et al., 2021). Drought also restricts the movement of nutrients in soil water, reducing their availability to trees and consequently impacting their growth and productivity (Bauke et al., 2022).

Changes in plant water-use and nutrient cycling can trigger feedback loops that magnify the effects of drought and heat stress. For instance, reduced plant cover can increase soil temperatures and further accelerate water loss and increase plant water demand (Haesen et al., 2023). On the other hand, increased atmospheric dryness or reduced soil moisture levels increase stomatal closure, which limits transpiration and leads to higher leaf temperatures that intensify heat stress on plants (Drake et al., 2018). Reduced transpiration and photosynthesis elevate surface temperatures and atmospheric CO<sub>2</sub> concentrations, altering local and regional climate patterns and intensifying the frequency and severity of extreme events (Humphrey et al., 2018). These effects vary significantly depending on forest type and species composition. Together with the characteristics of the extreme events themselves – such as their extent and severity – this variability complicates our understanding of how drought affects the functionality of different forest ecosystems (Gharun et al., 2020; Shekhar et al., 2023). These feedback loops highlight the urgent need to assess how climate extremes impact different forest types, which are crucial for sequestering significant portions of anthropogenic emissions. Our study aims to (1) quantify the extent and severity of the extreme conditions in 2022 – focusing on soil and atmospheric dryness – and compare them to those of two previous extreme years (2003, 2018), (2) quantify the responses of different forest types to drought in terms of canopy browning and photosynthesis, and (3) connect the functional characteristics of the forests with the canopy-level responses observed.

## 2 Methods

### 2.1 Meteorological dataset

We used Europe-wide gridded datasets covering daily mean air temperature ( $T_{\text{air}}$ , °C), daily mean relative humidity (RH, %), and daily mean soil moisture (SM, m<sup>3</sup> m<sup>-3</sup>) for the topsoil layer (0–7 cm depth), spanning 2000–2022. The study area encompasses longitudes from 11° W to 32° E and latitudes from 35.8 to 72° N, approximately 4.45 × 10<sup>6</sup> km<sup>2</sup>. We sourced the  $T_{\text{air}}$  and RH datasets from the E-OBS v27.0e dataset, which provides daily data at 0.1° × 0.1° spatial resolution (Cornes et al., 2018; Klein et al., 2002). We calculated daily mean vapour pressure deficit (VPD, kPa) from  $T_{\text{air}}$  and RH using Eq. (1) (Dee et al., 2011).

$$\text{VPD} = \left(1 - \frac{\text{RH}}{100}\right) \times 0.6107 \times 10^{\frac{17.27 \times T_{\text{air}}}{237.3 + T_{\text{air}}}} \quad (1)$$

The topsoil SM dataset was extracted from the most recent reanalysis data from ECMWF's (European Centre for Medium-Range Weather Forecasts) new land component of the fifth generation of the European reanalysis (ERA5-Land) dataset (daily at 0.1° × 0.1° resolution; Muñoz-Sabater et al., 2021). ERA5-Land provides soil moisture (SM) data at an

hourly interval with a spatial resolution of  $0.1^\circ \times 0.1^\circ$ . For our analysis, we aggregated the hourly SM data into daily averages. Recent validation studies using in situ measurements and satellite data have confirmed the high accuracy of surface SM simulations from ERA5-Land (Albergel et al., 2012; Lal et al., 2022; Muñoz-Sabater et al., 2021). Additionally, SM data from ERA5-Land have been utilized to investigate drought and global SM patterns (see Lal et al., 2023; Shekhar et al., 2024a). We resampled the  $T_{\text{air}}$ , VPD, and SM data from daily ( $0.1^\circ \times 0.1^\circ$ ) to 8 d ( $0.05^\circ \times 0.05^\circ$ ) intervals to align with the temporal and spatial resolutions of the vegetation response dataset (see below).

## 2.2 Forest canopy response dataset

In order to assess the forest canopy response to drought stress, we used two satellite-based proxies:

1. The first is the structure-based  $\text{NIR}_v$  (near-infrared reflectance of vegetation) index derived from MODIS (Moderate Resolution Imaging Spectroradiometer; 8 d  $500\text{ m} \times 500\text{ m}$  MOD09Q1 v6.1 product), which is calculated using surface spectral reflectance at near-infrared band ( $R_{\text{NIR}}$ ) and the red band ( $R_{\text{Red}}$ ), as shown in Eq. (2) (Badgley et al., 2017). The calculated  $\text{NIR}_v$  at 500 m resolution was aggregated to a  $0.05^\circ \times 0.05^\circ$  resolution (daily) by averaging.

$$\text{NIR}_v = R_{\text{NIR}} \times \frac{R_{\text{NIR}} - R_{\text{Red}}}{R_{\text{NIR}} + R_{\text{Red}}} \quad (2)$$

2. The second is the physiological-based reconstructed global OCO-2 (Observation Carbon Observatory 2) solar-induced fluorescence (GOSIF) dataset. Solar-induced fluorescence (SIF) is an energy flux (unit:  $\text{W m}^{-2} \mu\text{m sr}^{-1}$ ) reemitted as fluorescence by the chlorophyll *a* molecules in the plants during photosynthesis (Baker, 2008). Recent extensive research has established a strong link between solar-induced fluorescence (SIF) and vegetation photosynthesis, validating SIF as an effective proxy for ecosystem gross primary productivity (GPP) (Li et al., 2018; Magney et al., 2019; Shekhar et al., 2022). The GOSIF dataset was created by training a cubist regression tree model to fill the gaps in SIF retrievals from the OCO-2 satellite. This was done using MODIS enhanced vegetation index (EVI) and meteorological reanalysis data from MERRA-2 (Modern-Era Retrospective analysis for Research and Applications), which includes photosynthetically active radiation (PAR), VPD, and air temperature (see Li and Xiao, 2019). We downloaded the GOSIF dataset (v2) from the Global Ecology Data Repository ([http://data.globalecology.unh.edu/data/GOSIF\\_v2/](http://data.globalecology.unh.edu/data/GOSIF_v2/), last access: 25 July 2024). GOSIF information was available from 2000 to 2022 at 8 d temporal resolution with a spatial resolution of  $0.05^\circ \times 0.05^\circ$  (Li and Xiao, 2019).

GOSIF signals provide information about the physiological response of forest photosynthesis, while  $\text{NIR}_v$  (a recently developed vegetation index) signals provide information about the health status of the canopy.  $\text{NIR}_v$  is preferred over Normalized Difference Vegetation Index (NDVI) and EVI as it can isolate the vegetation signal, mitigate mixed-pixel issues, and partly address the influences of background brightness and soil contamination (Zhang et al., 2022). The two vegetation proxies used in this study are anticipated to offer complementary insights into the vegetation response to drought.

## 2.3 Land cover dataset

In this study, we focused on five different types of forests (and woodlands) across Europe, namely evergreen needle-leaf forest (ENF), evergreen broadleaf forest (EBF), deciduous broadleaf forest (DBF), mixed forest (MF), and woody savanna (WSA). The spatial distribution of the five different forest types across Europe is shown in Fig. 1. We used the yearly MODIS land cover product (MCD12C1 version 6.1 at  $0.05^\circ \times 0.05^\circ$  resolution) for the years of 2001, 2006, 2011, 2016, and 2021 to extract total areas covered by each forest type. Area of each grid cell was calculated using trigonometric equations, considering the latitudinal and longitudinal variations arising due to Earth's spherical shape (ellipsoid). Only areas that were consistently identified as each forest type over the 5-year period were included in the analysis. This means that only pixels that were common across these 5 years and had more than 50 % of the  $0.05^\circ \times 0.05^\circ$  pixel area identified as forest were selected. The forested areas selected for this study encompassed  $907\,875\text{ km}^2$ , which represents approximately 24 % of Europe's total land area. Out of the total area, about 23 % ( $206\,212\text{ km}^2$ ) was dominated by ENF, distributed largely across Northern Europe (NEU). Approximately 1 % ( $7000\text{ km}^2$ ) of the area was dominated by EBFs, located entirely in Mediterranean Europe (MED), and about 10 % ( $92\,209\text{ km}^2$ ) was dominated by DBFs, which were largely distributed across MED. Approximately 20 % ( $174\,934\text{ km}^2$ ) of the total forested area was dominated by MFs, largely dominating Central Europe (CEU), and about 47 % ( $427\,529\text{ km}^2$ ) was dominated by WSA, mostly found in NEU (Fig. 1).

## 2.4 Drought detection and statistical data analysis

The focus of our analysis was on the summer months during the three extreme years of 2003, 2018, and 2022. For this purpose, we subset VPD, soil moisture (SM), and both vegetation proxies ( $\text{NIR}_v$  and GOSIF) for the months of June, July, and August (JJA), which consisted of fourteen 8 d periods for each forested pixel between 2000 and 2022. We restricted our analysis to the months of June–July–August, so our study is (1) comparable with existing studies focused on the summer drought and (2) able to capture the peak of the

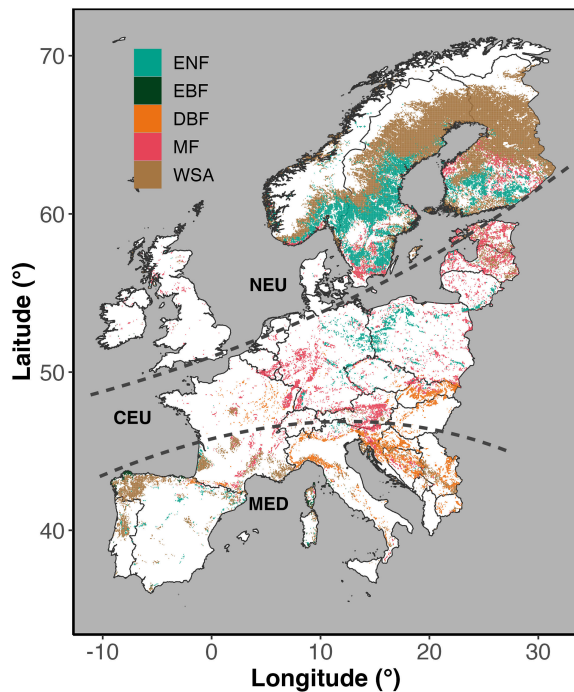


**Figure 1.** Spatial coverage of forests (ENF – evergreen needle-leaf forest; EBF – evergreen broadleaf forest; DBF – deciduous broadleaf forest; MF – mixed forest) and woodlands (WSA – woody savannas) across Europe. Areas are differentiated into Northern Europe (NEU), Central Europe (CEU), and Mediterranean Europe (MED) following Markonis et al. (2021). The map is based on the MODIS land cover product MCD12C1 (version 6.1).

warm and dry conditions across Europe that would be most stressful for the vegetation functioning, from the perspective of heat and water supply.

To account for the impact of the observed greening trend across Europe on vegetation proxy anomalies during the extreme years (2003, 2018, and 2022), we applied a detrending process to the summer mean  $\text{NIR}_v$  and GOSIF data. This detrending was performed pixel-wise from 2000 to 2022 using a simple linear regression model (Buras et al., 2020). We then calculated pixel-wise standardized summer anomalies, expressed as  $z$  scores ( $\text{Var}_z$ ), for all variables – VPD, SM, and the detrended  $\text{NIR}_v$  and GOSIF (hereafter referred to as  $\text{NIR}_v$  and GOSIF) – for each year, including the extreme years, using Eq. (3).

$$\text{Var}_z \text{ (unitless)} = \frac{\text{Var} - \text{Var}_{\text{mean}}}{\text{Var}_{\text{SD}}}, \quad (3)$$

where  $\text{Var}_{\text{mean}}$  and  $\text{Var}_{\text{SD}}$  are mean and standard deviation of any variable over the 2000–2022 period.

In drought identification studies, classification of “normal” (not to be confused with normal distribution), “drought” (used synonymously with “dry”), or “wet” is largely done using a standardized index, such as SPI (Standardized Precipitation Index), SPEI (Standardized Precipitation Evapotran-

spiration Index), or  $z$  score (among others) (see Mishra and Singh, 2011). All studies that use a standardized index for classification classify “normal” conditions when the index is between  $-1$  and  $1$ , “below normal” conditions when the index is  $< -1$ , and “above normal” conditions when the index  $> 1$  (Jain et al., 2015; Wable et al., 2019; Dogan et al., 2012; Tsakiris and Vangelis, 2005). In this study, we classified drought conditions as occurring when soil moisture is below normal ( $\text{SM}_z < -1$ ) and VPD is above normal ( $\text{VPD}_z > 1$ ), indicating both soil and atmospheric dryness. This threshold-based approach using standardized anomalies aligns with established methods for drought identification and is pertinent for studying drought impacts on forests. Both soil moisture and VPD directly affect vegetation functioning, making them effective proxies for identifying environmental constraints on plant physiological performance. Furthermore, such a classification as normal (and thus above normal and below normal, used in this study) based on  $z$  scores (also called standardized anomalies) can be done for any meteorological and/or response variables, such as  $\text{NIR}_v$  and GOSIF as done in this study, making the narration of results coherent across different variables.

We used the Pearson correlation coefficient ( $r$ ) and partial correlation coefficients ( $\text{Pr}$ ) to understand the spatial (across space for each year) and temporal (during each year) correlation of GOSIF and  $\text{NIR}_v$  anomalies with SM and VPD anomalies (Dang et al., 2022). We calculated the partial correlation coefficient using Eqs. (4)–(7):

$$\begin{aligned} \text{Pr}(\text{GOSIF}, \text{SM}) &= \frac{r(\text{GOSIF}, \text{SM}) - r(\text{GOSIF}, \text{VPD}) \times r(\text{SM}, \text{VPD})}{\sqrt{1 - r(\text{GOSIF}, \text{VPD})^2} - \sqrt{1 - r(\text{SM}, \text{VPD})^2}}, \quad (4) \end{aligned}$$

$$\begin{aligned} \text{Pr}(\text{GOSIF}, \text{VPD}) &= \frac{r(\text{GOSIF}, \text{VPD}) - r(\text{GOSIF}, \text{SM}) \times r(\text{SM}, \text{VPD})}{\sqrt{1 - r(\text{GOSIF}, \text{SM})^2} - \sqrt{1 - r(\text{SM}, \text{VPD})^2}}, \quad (5) \end{aligned}$$

$$\begin{aligned} \text{Pr}(\text{NIR}_v, \text{SM}) &= \frac{r(\text{NIR}_v, \text{SM}) - r(\text{NIR}_v, \text{VPD}) \times r(\text{SM}, \text{VPD})}{\sqrt{1 - r(\text{NIR}_v, \text{VPD})^2} - \sqrt{1 - r(\text{SM}, \text{VPD})^2}}, \quad (6) \end{aligned}$$

$$\begin{aligned} \text{Pr}(\text{NIR}_v, \text{VPD}) &= \frac{r(\text{NIR}_v, \text{VPD}) - r(\text{NIR}_v, \text{SM}) \times r(\text{SM}, \text{VPD})}{\sqrt{1 - r(\text{NIR}_v, \text{SM})^2} - \sqrt{1 - r(\text{SM}, \text{VPD})^2}}. \quad (7) \end{aligned}$$

### 3 Results

#### 3.1 Severity of the 2022 summer drought compared to 2018 and 2003

Figure 2 shows the extent and magnitude of anomalies ( $z$  score) of VPD and top-layer (0–7 cm) soil moisture content during the summer months in 2003, 2018, and 2022 across Europe. In summer 2022, particularly southern regions of Europe experienced the most pronounced increase in atmospheric ( $z$  score  $> 1$ ) and soil dryness ( $z$  score  $< -1$ )

(Fig. 2), while in 2018 we observed the most widespread VPD and SM anomalies in northern Europe (Fig. 2).

Figure 3 shows the intensity of atmospheric and soil drought via  $z$ -score values of VPD and SM anomalies over the summer months (JJA) in 2003, 2018, and 2022. The total affected area displayed in Fig. 3 is the sum of all pixels within the given  $z$ -score bin during the summer period where  $z$  scores are averaged for each bin for the summer period. Restricted to forested areas, atmospheric and soil drought scores were 55 % and 58 % more extensive in 2018 compared to 2022, and in both years they were more extensive than in 2003 (Fig. 3). In 2022, 28 Mha of forested areas in Europe was affected by an extremely high VPD ( $z$  score  $> 1$ ), while in 2018 an area of 63 Mha was affected by such extreme conditions. In 2022, 21 Mha of forested area was affected by an extremely low soil moisture content ( $z$  score  $< -1$ ), while in 2018 an area of 50 Mha of forest in Europe was affected by such extreme conditions. In 2003, an area of 25 Mha was affected by extremely dry air, and a similar area was affected by extremely dry soil (Fig. 3). A comparison of soil drought detected from SM at 0–100 cm showed a similar result in terms of drought severity and spatial coverage; thus, we used SM at the 0–7 cm soil layer for our analysis (see Fig. S1).

### 3.2 Forest canopy response to the 2022 drought

The intensities of GOSIF and  $\text{NIR}_v$  anomalies over the summer months (JJA) in 2003, 2018, and 2022 are displayed in Fig. 4. The extent shown in Fig. 4 is the sum of all pixels within the given  $z$ -score bin during the summer period ( $z$  scores are averaged for each bin). Compared to 2018, the extremely dry conditions in 2022 led to a 30 % increase in forested areas that exhibited declined photosynthesis (17 Mha in 2022 compared to 12 Mha in 2018) (Fig. 4). The extent of the canopy browning observed in 2022 was similar to 2018, which in both years was 120 % of the extent of observed canopy browning in 2003 (11 Mha compared to 5 Mha observed in 2003) (Fig. 4).

Figure 5a shows the GOSIF anomalies ( $z$  score) across all forested areas in Europe. The intensity and extent of the GOSIF anomalies during the summer months (JJA) in each year are shown for different forest types in Fig. 5b. Across specific forest types, DBFs showed the largest negative GOSIF anomaly in 2022, but the ENFs showed a positive GOSIF anomaly in 2022, both in terms of magnitude and in terms of the spatial extent of negative GOSIF anomalies (Fig. 5).

Figure 6a shows the anomalies of  $\text{NIR}_v$  (average  $z$  score over the summer months) across all forested areas in Europe. The intensity and extent of the  $\text{NIR}_v$  anomalies during the summer months (JJA) in each year are shown for different forest types in Fig. 6b. In terms of canopy browning response ( $\text{NIR}_v$  anomalies), the largest negative  $\text{NIR}_v$  anomalies in 2022 were observed in southern Europe (Fig. 6). The largest negative  $\text{NIR}_v$  anomalies (indicated by the maximum

anomaly) were observed in DBFs in 2022, fitting with the declined GOSIF signals. The ENFs showed positive  $\text{NIR}_v$  anomalies in 2022, in terms of magnitude, spatial coverage, and percent of total area affected (Fig. 6).

### 3.3 Relationship between GOSIF and $\text{NIR}_v$

In general, the values of  $\text{NIR}_v$  and GOSIF were highly correlated (Fig. S2). The anomalies of  $\text{NIR}_v$  and GOSIF were most correlated across WSAs ( $r^2 = 0.73$  in 2018) and least correlated across the ENFs (Fig. S2). Figure 7 shows the spatial regression between standardized GOSIF anomalies with (a) VPD and (b) SM, and Fig. 8 shows the spatial regression between standardized  $\text{NIR}_v$  anomalies with (a) VPD and (b) SM over the drought areas in summers 2003, 2018, and 2022. With the increase in VPD (i.e. increased atmospheric dryness), GOSIF values declined across all forest types, across all years (except in 2022 in the WSA), and in 2018 and 2022 in EBFs (Fig. 7). With the decrease in soil moisture (i.e. increased soil dryness), GOSIF values also declined overall ( $r^2 = 0.34$ ) but not as strongly as with the increase in air dryness ( $r^2 = 0.39$ ) (Fig. 7). Across different forest types, GOSIF responded most strongly to VPD anomalies in the MFs (mean  $r^2 = 0.48$ ) and responded most directly to changes in the soil moisture in the WSA (Fig. 7).

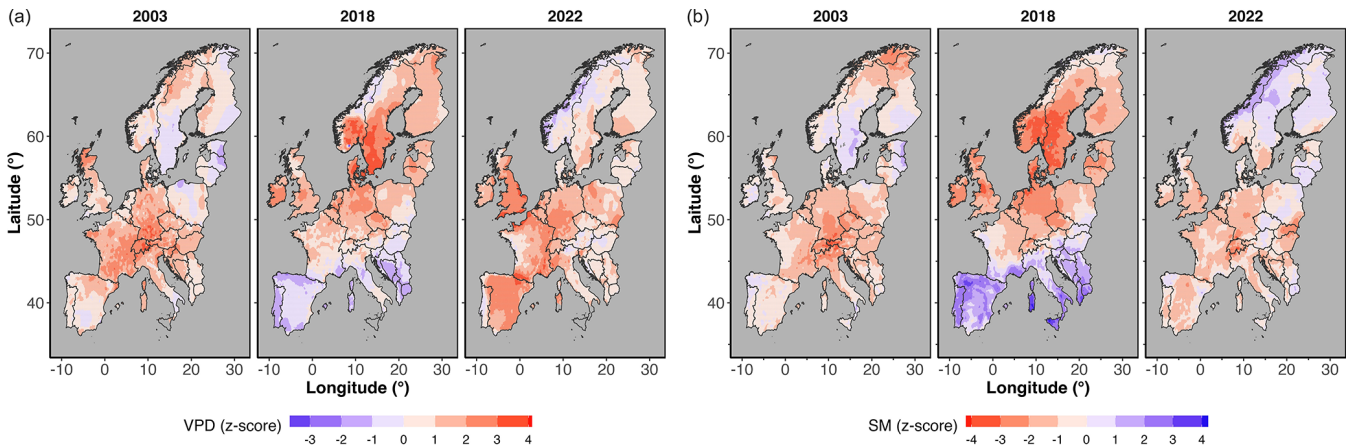
Between VPD and SM, in general GOSIF anomalies were more correlated with VPD than with SM anomalies, and the decline in VPD correlated well with the larger GOSIF decline that we observed in DBFs in 2022 and in ENFs in 2003 (Fig. 7). Under typical conditions (regardless of drought), GOSIF's response to both air dryness and soil moisture anomalies was more pronounced than the response of  $\text{NIR}_v$  ( $r^2 = 0.39$  with GOSIF compared to  $r^2 = 0.29$  for  $\text{NIR}_v$ ) (Figs. 7 and 8).

Figure 9 shows the partial correlation coefficient between GOSIF with SM and VPD during summer months (JJA) for areas identified as affected (Fig. 9a) and not affected (Fig. 9b) by drought. The SM and VPD values across all forest types correlated well, but across DBFs the dryness in the atmosphere and the dryness in the soil were most correlated (Fig. 9). Regarding canopy response to VPD, ENF exhibited the strongest reaction to changes in atmospheric dryness (Fig. 9).

## 4 Discussion

### 4.1 Severity of the 2022 summer drought

Although the years 2003, 2018, and 2022 are all categorized as “extreme”, the specific characteristics of the extreme conditions varied significantly among these years. For example, in 2003, widespread negative anomalies in soil moisture signalled a significant soil drought, whereas in 2022 widespread positive VPD anomalies indicated a notably drier atmosphere (Fig. 3). It is important to note that ERA5-Land



**Figure 2.** Standardized summer (JJA) anomalies ( $z$  score) of mean vapour pressure deficit (VPD) and top-layer (0–7 cm depth) soil moisture (SM) in 2003, 2018, and 2022 across the region of Europe.

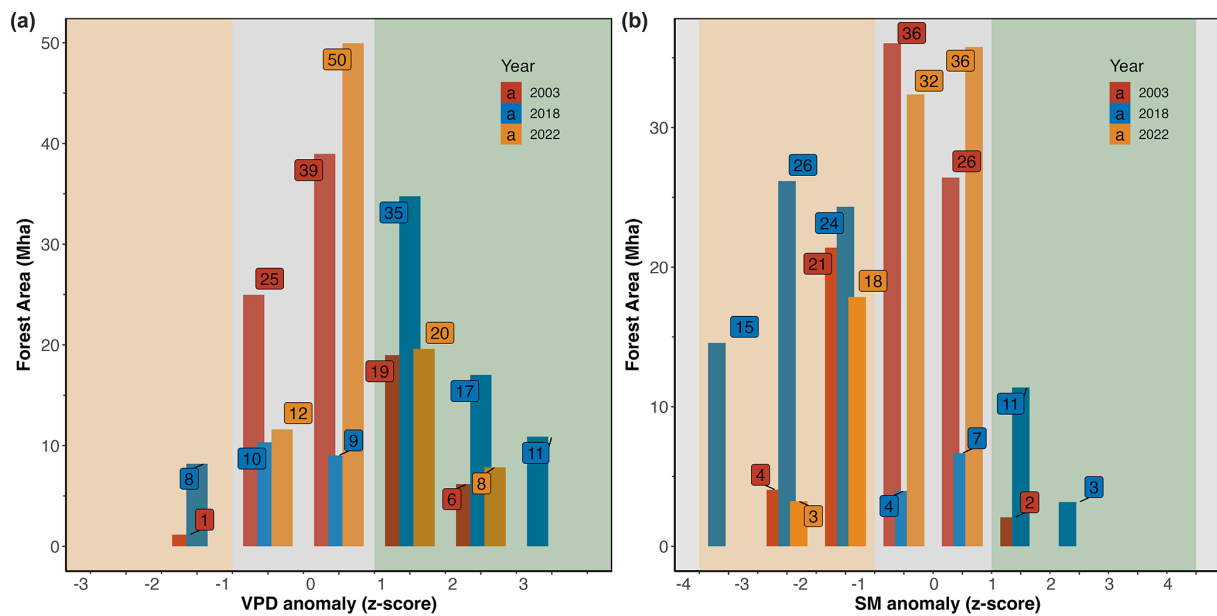


**Figure 3.** Intensity ( $z$  score) and extent (area affected, Mha) of (a) VPD and (b) SM anomalies across forested areas during the summer months (JJA). The  $z$  scores, values from  $-1$  and  $1$ , are considered normal (within 1 standard deviation of the mean). The shaded orange area marks below-normal conditions, and the shaded green area marks above-normal conditions.

datasets have been shown to underestimate the extent of European heat waves in 2003, 2010, and 2018 (Duveiller et al., 2023), partly due to the use of a static leaf area index in their modelling framework. Consequently, the SM droughts in the years 2003, 2018, and 2022 may be more severe than indicated by our study, suggesting that our results might be somewhat conservative. The extensive summer drought in 2022 primarily impacted southern Europe, in contrast to the 2003 summer drought that affected central Europe and the 2018 drought that extended to Central and Northern Europe (Fig. 2) (Bastos et al., 2020). Consequently, the severe dry conditions in 2022 resulted in an average de-

cline in GOSIF across forests that was 30 % more widespread compared to 2018 and 60 % more widespread compared to 2003 (Fig. 4). These above-normal dry conditions during the summer reduced the photosynthetic capacity of plants and, consequently, the ecosystem's ability to absorb carbon from the atmosphere (Peters et al., 2018; van der Woude et al., 2023). Although the atmospheric and soil droughts in 2018 were more extensive and severe compared to 2022 (as indicated by the maximum observed  $z$  scores), the adverse impact on forests, as reflected by the decline in GOSIF, was greater in 2022.

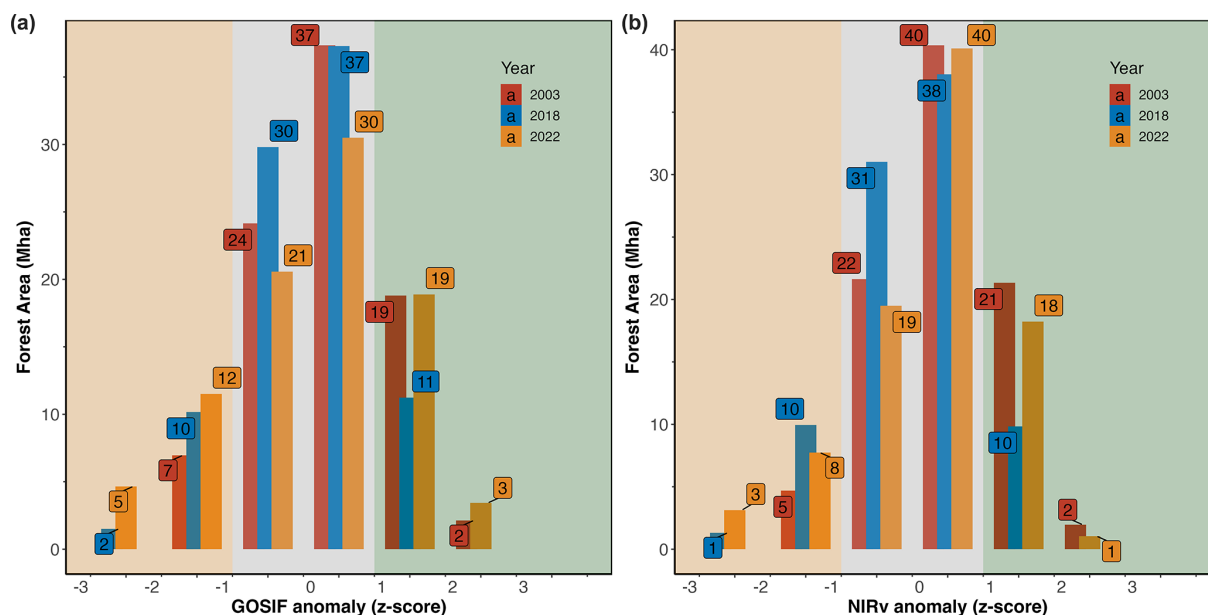


**Figure 4.** Intensity ( $z$  score) and extent (area affected, Mha) for (a) GOSIF and (b)  $\text{NIR}_v$  anomalies across forested areas during the summer months (JJA). The  $z$  scores, values from  $-1$  and  $1$ , are considered normal (within 1 standard deviation of the mean). The shaded orange area marks below-normal conditions, and the shaded green area marks above-normal conditions.

#### 4.2 Canopy response to soil versus atmospheric dryness

The GOSIF dataset used in this study has been shown to be a reliable proxy for vegetation gross productivity, as demonstrated by comparisons with ground-based flux measurements (Shekhar et al., 2022; Pickering et al., 2022). It is important to note that GOSIF estimates are derived from a machine learning model trained with OCO-2 SIF observations, MODIS EVI data, and meteorological reanalysis data. As a result, the meteorological data used in our analyses are not entirely independent of the SIF data. However, this overlap is unlikely to impact our findings. A recent study that compared GOSIF with original OCO-2 data to assess the impacts of the 2018 US drought found similar responses to drought between the two datasets (Li et al., 2020).

$\text{NIR}_v$  and SIF signals are correlated well and effectively capture seasonal patterns in GPP (Mengistu et al., 2021). Although the strength of their relationship can vary with time, location, and forest type (see Fig. S2), reductions in SIF signals are directly associated with decreased photosynthesis. While both SIF and  $\text{NIR}_v$  are reliable indicators of canopy responses to extreme climate events, SIF is more responsive to short-term climatic changes (Fig. 7).

Our analysis showed that, across different regions, GOSIF anomalies corresponded more strongly to increased atmospheric dryness than to increased soil dryness (Fig. 7). This supports the understanding that vapour pressure deficit plays a larger role in controlling SIF signals for trees over shorter timescales than soil moisture (Pickering et al., 2022). Over

shorter time frames, trees can often mitigate soil moisture deficits through mechanisms within the rooting zone and by accessing deeper water sources, whereas there is no such buffer for the impact of atmospheric dryness on tree canopies.

Ground-based observations in forest ecosystems, including both ecosystem- and tree-level measurements, have shown that atmospheric dryness can constrain canopy gas exchange, even when soil moisture is not limited (Gharun et al., 2014; Fu et al., 2022; Shekhar et al., 2024b). These findings highlight the importance of considering atmospheric dryness as a limiting factor for tree photosynthesis during extremely dry conditions and demonstrate the rapid response of various canopy types to increased levels of environmental dryness.

#### 4.3 Canopy response to drought across different forest types

The spread of drought, measured as the total area across  $z$  scores, exhibited distinct patterns in different years, leading to varied responses of different forest types to the climatic anomalies. The impact of drought on forests can significantly differ depending on the forest type, tree species, species composition, and past exposure to extreme conditions (Arthur and Dech 2016; Chen et al., 2022). Our analysis showed that conditions in summer 2022 reduced vegetation functioning across DBFs the most, as was indicated by declined GOSIF signals (Fig. 5). While DBFs were most negatively affected by the extreme conditions in 2022, ENFs distributed in northern regions of Europe were not exposed to extremely dry

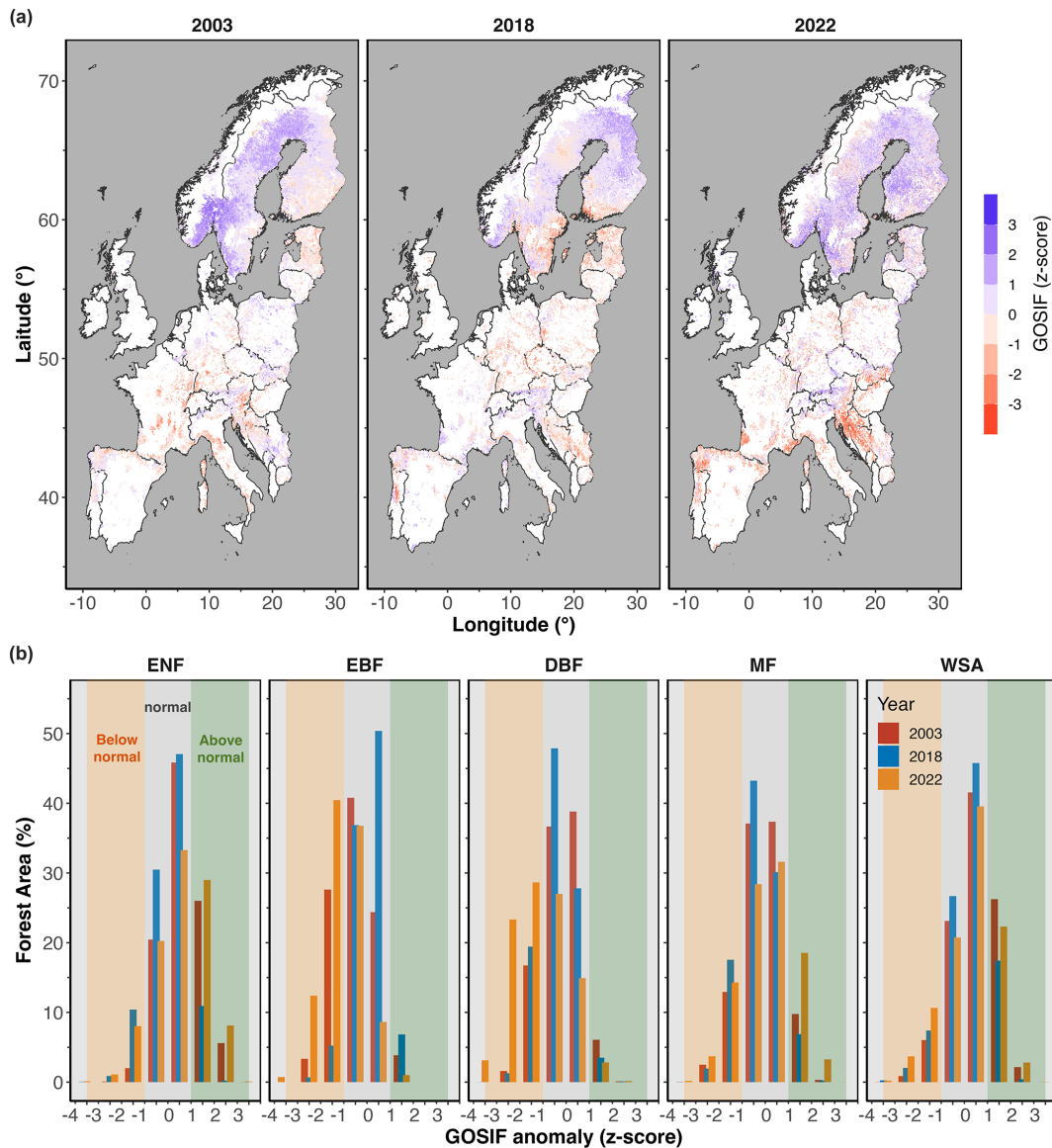


**Figure 5.** (a) GOSIF anomaly (in terms of  $z$  score) across Europe and (b) area coverage (in terms of percentage of total area for each forest type) during the summer months (JJA) in 2003, 2018, and 2022. The shaded orange area marks below-normal conditions, and the shaded green area marks above-normal conditions. White areas on the map mark non-forested regions.

conditions in 2022, and they even showed enhanced canopy greening and GOSIF signals by benefiting from the episodic warming (Forzieri et al., 2022). Under similar drought conditions, the mechanisms to cope with the level of drought stress vary largely among forest types, and they depend on a combination of characteristics that control water loss through the coordination of stomatal regulation, hydraulic architecture, and root characteristics (e.g. rooting depth, root distribution, root morphology) (Gharun et al., 2020; Peters et al., 2023). Stomata of trees exhibit a high sensitivity to VPD fluctuations, causing a reduction in stomatal conductance as VPD increases, which, in turn, limits the exchange of  $\text{CO}_2$  with the atmosphere during photosynthesis (Bonafant and Guehl in

2011; Li et al., 2023). Different tree species show varying degrees of sensitivity in their stomatal responses to atmospheric dryness (Oren et al., 1999). For example, ring-porous species tend to maintain robust gas exchange under dry conditions, while diffuse-porous species, like those in ENFs, exhibit stronger stomatal regulation, reducing stomatal conductance as water availability decreases (Klein, 2014). This variability places plants on a spectrum of drought tolerance, reflecting their specific water relation strategies and leading to different responses among forests in similar climatic regions.



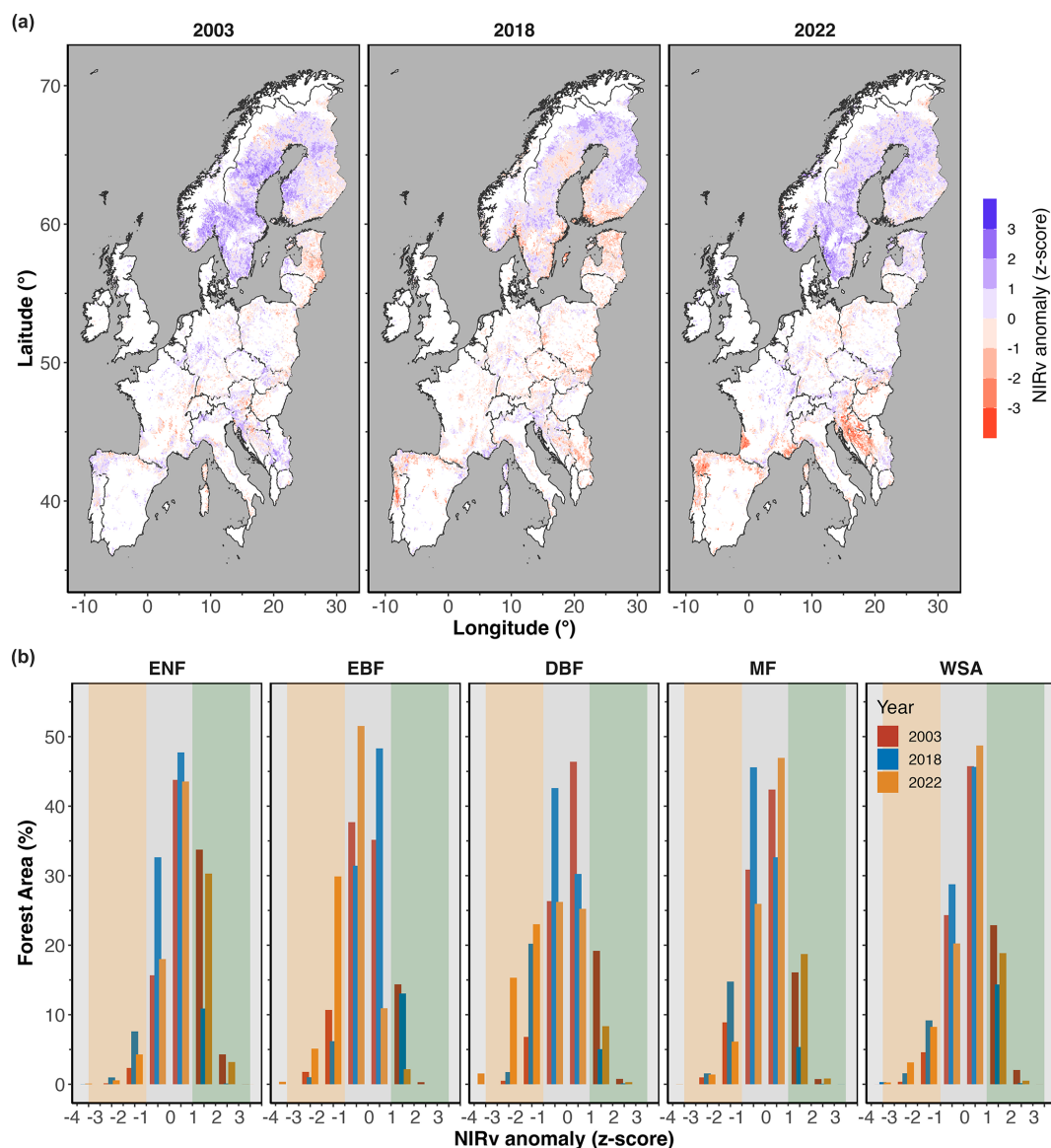


**Figure 6.** (a) NIR<sub>v</sub> anomaly (in terms of  $z$  score) across Europe, and (b) area coverage (in terms of percentage of total area for each forest type) during the summer months (JJA) in 2003, 2018, and 2022. In panel (b), the shaded orange area marks below-normal conditions, and the shaded green area marks above-normal conditions. White areas on the map mark non-forested regions.

#### 4.4 Vulnerability of forests to more frequent drought

The increased canopy damage observed in 2022, despite less severe conditions compared to the previous extreme year, suggests a lasting impact on forest canopies that could lead to a decline in forest resilience in the face of more frequent drought events (Forzieri et al., 2022). A potential decline in the resilience of forests has significant implications for vital ecosystem services, including the forest's capacity to mitigate climate change. Consequently, there is an urgent need to consider these trends when formulating robust forest-based mitigation strategies. This need is especially critical, given that future projections are indicating that the frequency and

intensity of extreme dryness across Europe will more than triple by the end of the 21st century (Shekhar et al., 2024a). In this context, it is increasingly important to investigate the vulnerability of forests to external perturbations and to develop mitigation strategies tailored to site-specific ecophysiological and environmental factors that influence forest resilience to drought. Effective management strategies should be based on an understanding of these factors to mitigate the legacy effects of drought (McDowell et al., 2020; Wang et al., 2023; Shekhar et al., 2024b).

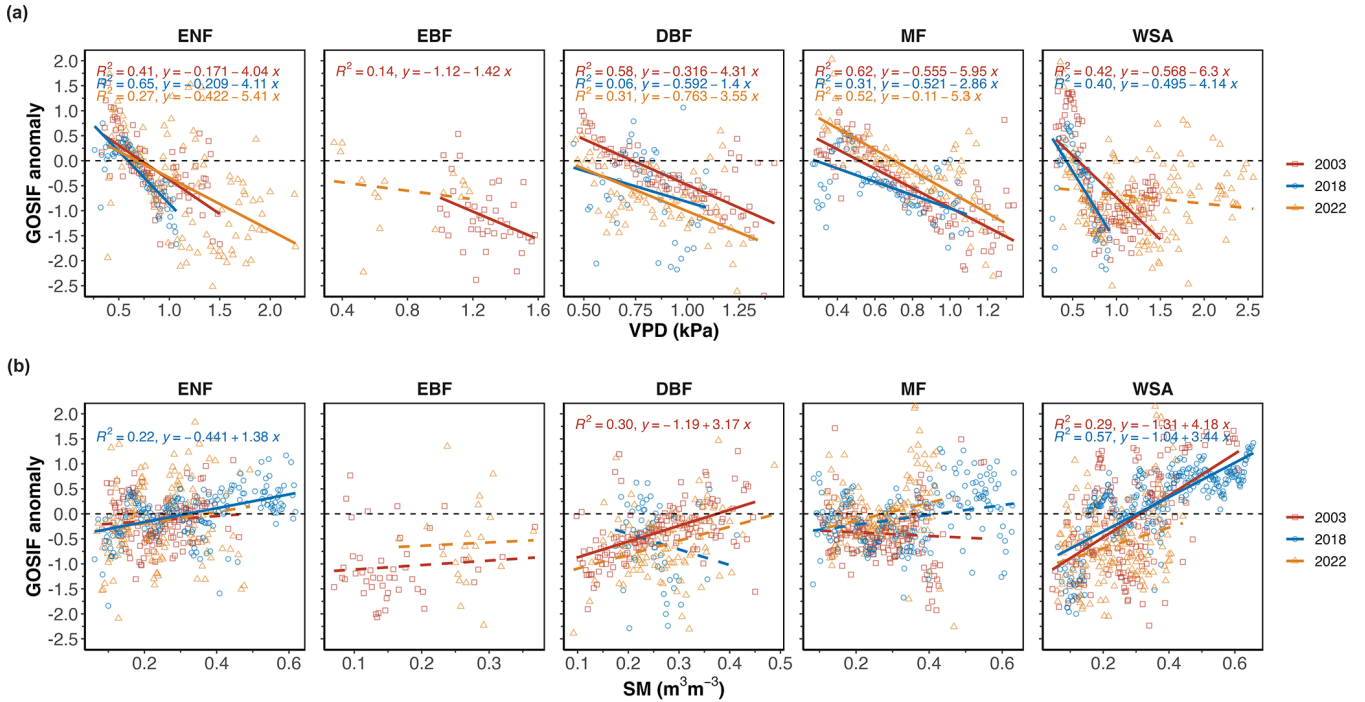


**Figure 7.** Spatial regression between standardized GOSIF anomalies with (a) VPD and (b) SM over the drought areas during the summer months (JJA) in 2003, 2018, and 2022. Dashed lines mark a non-significant relationship ( $p > 0.05$ ).

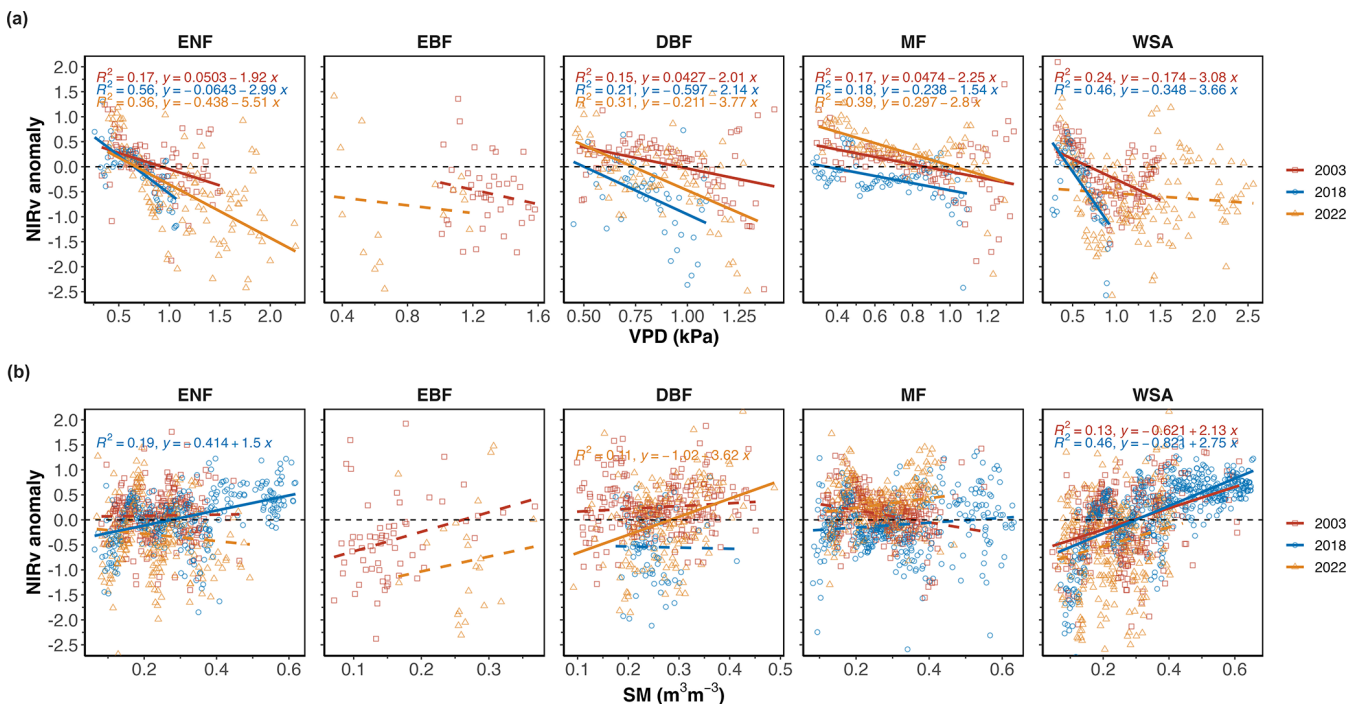


**Figure 8.** Spatial (over all pixels) regression between standardized NIRv anomalies with (a) VPD and (b) SM over the drought areas and normal areas in 2003, 2018, and 2022 during the summer months (JJA).

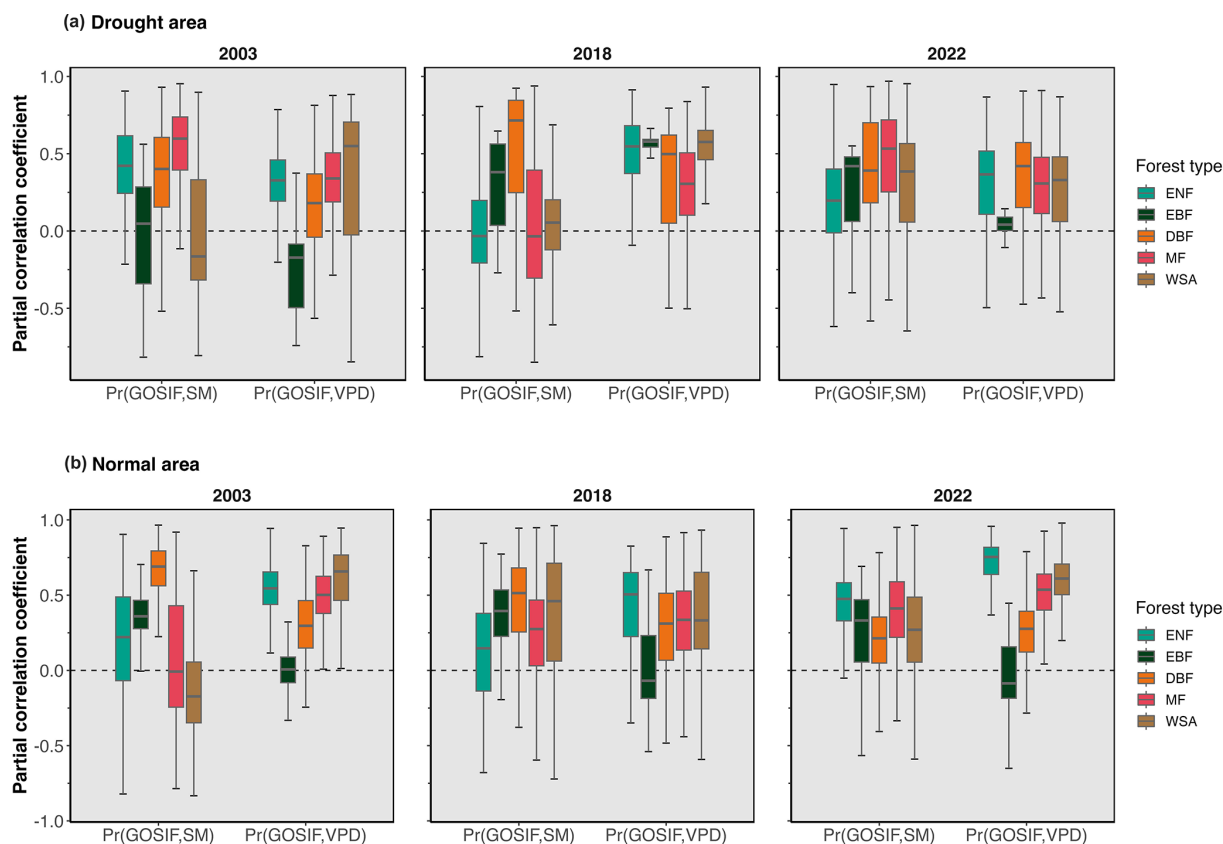


**Figure 9.** Temporal partial correlation coefficient of GOSIF with the absolute values of SM and VPD during the summer months (JJA) in 2003, 2018, and 2022 for detected (a) drought areas and (b) normal areas. A comparable figure for  $\text{NIR}_v$  can be found in Fig. S3.

## 5 Conclusions

The severity of the 2022 summer drought, marked by increased atmospheric dryness, significantly compromised the photosynthetic capacity of trees, leading to widespread declines in vegetation functioning, especially in deciduous broadleaf forests. Our findings underscore the importance of considering atmospheric dryness as a critical factor influencing canopy responses during extreme climatic events, alongside soil moisture deficits. Despite less severe overall conditions compared to previous extreme years, the greater canopy damage observed in 2022 suggests a growing vulnerability of forests to drought. This raises concerns about the future climate mitigation capacity of forest ecosystems, particularly as projections indicate a continued increase in the frequency and intensity of extreme dryness across Europe.

**Data availability.** The R scripts used for the data analyses and plots are available upon request from the corresponding author.

**Supplement.** The supplement related to this article is available online at: <https://doi.org/10.5194/bg-21-5481-2024-supplement>.

**Author contributions.** MG, AS, and NB conceptualized the study. AS, JX, and XL performed data processing. MG and AS contributed to data analyses. MG, AS, JX, and XL contributed to paper writing (revision and editing).

**Competing interests.** At least one of the (co-)authors is a guest member of the editorial board of *Biogeosciences* for the special issue “Drought, society, and ecosystems (NHESS/BG/GC/HES inter-journal SI)”. The peer-review process was guided by an independent editor, and the authors also have no other competing interests to declare.

**Disclaimer.** Publisher’s note: Copernicus Publications remains neutral with regard to jurisdictional claims made in the text, published maps, institutional affiliations, or any other geographical representation in this paper. While Copernicus Publications makes every effort to include appropriate place names, the final responsibility lies with the authors.

**Special issue statement.** This article is part of the special issue “Drought, society, and ecosystems (NHESS/BG/GC/HES inter-journal SI)”. It is not associated with a conference.

*Acknowledgements.* Ankit Shekhar acknowledges financial support from the Swiss National Science Foundation (SNF) through the EcoDrive project (grant no. IZCOZO\_198094). Jingfeng Xiao acknowledges funding from the National Science Foundation (NSF) under the Macrosystems Biology and NEON-Enabled Science program (grant no. DEB-2017870).

*Financial support.* This research has been supported by the Schweizerischer Nationalfonds zur Förderung der Wissenschaftlichen Forschung (grant no. IZCOZO\_198094) and the National Science Foundation (NSF) (Macrosystem Biology and NEON-Enabled Science programme: DEB-2017870).

*Review statement.* This paper was edited by Giulia Vico and reviewed by two anonymous referees.

## References

- Albergel, C., De Rosnay, P., Balsamo, G., Isaksen, L., and Munoz-Sabater, J.: Soil moisture analyses at ECMWF: evaluation using global ground-based in situ observations, *J. Hydrometeorol.*, 13, 1442–1460, 2012.
- Anjileli, H., Huning, L. S., and Moftakhari, H.: Extreme heat events heighten soil respiration, *Sci. Rep.*, 11, 6632, <https://doi.org/10.1038/s41598-021-85764-8>, 2021.
- Arthur, C. M. and Dech, J. P.: Species composition determines resistance to drought in dry forests of the Great Lakes – St. Lawrence forest region of central Ontario, *J. Veg. Sci.*, 27, 914–925, 2016.
- Badgley, G., Field, C. B., and Berry, J. A.: Canopy near-infrared reflectance and terrestrial photosynthesis, *Sci. Adv.*, 3, e1602244, <https://doi.org/10.1126/sciadv.1602244>, 2017.
- Baker, N. R.: Chlorophyll Fluorescence: A Probe of Photosynthesis In Vivo, *Annu. Rev. Plant Biol.*, 59, 89–113, <https://doi.org/10.1146/annurev.arplant.59.032607.092759>, 2008.
- Bastos, A., Fu, Z., Ciais, P., Friedlingstein, P., Sitch, S., Pongratz, J., Weber, U., Reichstein, M., Anthoni, P., Arneth, A., Haverd, V., Jain, A., Joetzjer, E., Knauer, J., Lienert, S., Loughran, T., McGuire, P. C., Obermeier, W., Padrón, R. S., Shi, H., Tian, H., Viovy, N., and Zaehle, S.: Impacts of extreme summers on European ecosystems: a comparative analysis of 2003, 2010 and 2018, *Philos. T. R. Soc. B*, 375, 20190507, <https://doi.org/10.1098/rstb.2019.0507>, 2020.
- Bauke, S. L., Amelung, W., Bol, R., Brandt, L., Brüggemann, N., Kandeler, E., Meyer, N., Or, D., Schnepf, A., Schloter, M., Schulz, S., Siebers, N., von Sperber, C., and Vereecken, H.: Soil water status shapes nutrient cycling in agroecosystems from micrometer to landscape scales, *J. Plant Nutr. Soil Sci.*, 185, 773–792, <https://doi.org/10.1002/jpln.202200357>, 2022.
- Bonal, D. and Guehl, J.-M.: Contrasting patterns of leaf water potential and gas exchange responses to drought in seedlings of tropical rainforest species, *Funct. Ecol.*, 15, 490–496, 2011.
- Buras, A., Rammig, A., and Zang, C. S.: Quantifying impacts of the 2018 drought on European ecosystems in comparison to 2003, *Biogeosciences*, 17, 1655–1672, <https://doi.org/10.5194/bg-17-1655-2020>, 2020.
- Chen, Y., Vogel, A., and Wagg, C.: Drought-exposure history increases complementarity between plant species in response to a subsequent drought, *Nat. Commun.*, 13, 3217, <https://doi.org/10.1038/s41467-022-30954-9>, 2022.
- Choat, B., Brodribb, T. J., Brodersen, C. R., Duursma, R. A., López, R., and Medlyn, B. E.: Triggers of tree mortality under drought, *Nature*, 558, 531–539, <https://doi.org/10.1038/s41586-018-0240-x>, 2018.
- Copernicus Climate Change Service (C3S): State of the Climate in 2022 – Global climate highlights, <https://climate.copernicus.eu/globe-2022>, last access: 2 December 2024.
- Cornes, R. C., van der Schrier, G., van den Besselaar, E. J. M., and Jones, P. D.: An Ensemble Version of the E-OBS Temperature and Precipitation Data Sets, *J. Geophys. Res.-Atmos.*, 123, 9391–9409, <https://doi.org/10.1029/2017JD028200>, 2018.
- Dang, C., Shao, Z., Huang, X., Qian, J., Cheng, G., Ding, Q., and Fan, Y.: Assessment of the importance of increasing temperature and decreasing soil moisture on global ecosystem productivity using solar-induced chlorophyll fluorescence, *Glob. Change Biol.*, 28, 2066–2080, <https://doi.org/10.1111/gcb.16043>, 2022.
- Dee, D. P., Uppala, S. M., Simmons, A. J., Berrisford, P., Poli, P., Kobayashi, S., Andrae, U., Balmaseda, M. A., Balsamo, G., Bauer, P., Bechtold, P., Beljaars, A. C. M., van de Berg, L., Bidlot, J., Bormann, N., Delsol, C., Dragani, R., Fuentes, M., Geer, A. J., Haimberger, L., Healy, S. B., Hersbach, H., Hólm, E. V., Isaksen, L., Kållberg, P., Köhler, M., Matricardi, M., McNally, A. P., Monge-Sanz, B. M., Morcrette, J. J., Park, B. K., Peubey, C., de Rosnay, P., Tavolato, C., Thépaut, J. N., and Vitart, F.: The ERA-Interim reanalysis: configuration and performance of the data assimilation system, *Q. J. R. Meteorol. Soc.*, 137, 553–597, <https://doi.org/10.1002/qj.828>, 2011.
- Dogan, S., Berktaş, A., and Singh, V. P.: Comparison of multi-monthly rainfall-based drought severity indices, with application to semi-arid Konya closed basin, Turkey, *J. Hydrol.*, 470/471, 255–268, 2012.
- Drake, J. E., Tjoelker, M. G., Vårhammar, A., Medlyn, B. E., Reich, P. B., Leigh, A., Pfautsch, S., Blackman, C. J., López, R., Aspinwall, M. J., Crous, K. Y., Duursma, R. A., Kumarathunge, D., De Kauwe, M. G., Jiang, M., Nicotra, A. B., Tissue, D. T., Choat, B., and Atkin, O. K.: Trees tolerate an extreme heatwave via sustained transpirational cooling and increased leaf thermal tolerance, *Glob. Change Biol.*, 24, 2390–2402, <https://doi.org/10.1111/gcb.14037>, 2018.
- Duveiller, G., Pickering, M., Muñoz-Sabater, J., Caporaso, L., Boussetta, S., Balsamo, G., and Cescatti, A.: Getting the leaves right matters for estimating temperature extremes, *Geosci. Model Dev.*, 16, 7357–7373, <https://doi.org/10.5194/gmd-16-7357-2023>, 2023.
- Forzieri, G., Dakos, V., and McDowell, N. G.: Emerging signals of declining forest resilience under climate change, *Nature*, 608, 534–539, <https://doi.org/10.1038/s41586-022-04959-9>, 2022.
- Fu, Z., Ciais, P., and Prentice, I. C.: Atmospheric dryness reduces photosynthesis along a large range of soil water deficits, *Nat. Commun.*, 13, 989, <https://doi.org/10.1038/s41467-022-28652-7>, 2022.
- Gessler, A., Bottero, A., Marshall, J., and Arend, M.: The way back: recovery of trees from drought and its implication for acclimation, *New Phytol.*, 228, 1704–1709, <https://doi.org/10.1111/nph.16703>, 2020.

- Mengistu, A. G., Tsidu, G. M., Koren, G., Kooreman, M. L., Boersma, K. F., Tagesson, T., Ardö, J., Nouvellon, Y., and Peters, W.: Sun-induced fluorescence and near-infrared reflectance of vegetation track the seasonal dynamics of gross primary production over Africa, *Biogeosciences*, 18, 2843–2857, <https://doi.org/10.5194/bg-18-2843-2021>, 2021.
- Gharun, M., Vervoort, R. W., Turnbull, T. L., and Adams, M. A.: A test of how coupling of vegetation to the atmosphere and climate spatial variation affects water yield modelling in mountainous catchments, *J. Hydrol.*, 514, 202–213, <https://doi.org/10.1016/j.jhydrol.2014.04.037>, 2014.
- Gharun, M., Hörtnagl, L., Paul-Limoges, E., Ghiasi, S., Feigenwinter, I., Burri, S., Marquardt, K., Etzold, S., Zweifel, R., Eugster, W., and Buchmann, N.: Physiological response of Swiss ecosystems to 2018 drought across plant types and elevation, *Philos. T. R. Soc. B*, 375, 20190521, <https://doi.org/10.1098/rstb.2019.0521>, 2020.
- Gourlez de la Motte, L., Beauclaire, Q., Heinesch, B., Cuntz, M., Foltýnová, L., Šigut, L., Kowalska, N., Manca, G., Ballarin, I. G., Vincke, C., Roland, M., Ibrom, A., Lousteau, D., Siebicke, L., Neiryink, J., and Longdoz, B.: Non-stomatal processes reduce gross primary productivity in temperate forest ecosystems during severe edaphic drought, *Philos. T. R. Soc. B*, 375, 20190527, <https://doi.org/10.1098/rstb.2019.0527>, 2020.
- Haesen, S., Lembrechts, J. J., De Frenne, P., Lenoir, J., Aalto, J., Ashcroft, M. B., Kopecký, M., Luoto, M., Maclean, I., Nijs, I., Niittynen, P., van den Hoogen, J., Arriga, N., Brůna, J., Buchmann, N., Čiliak, M., Collalti, A., De Lombaerde, E., Descombes, P., and Van Meerbeek, K.: Forest-Clim – Bioclimatic variables for microclimate temperatures of European forests, *Glob. Change Biol.*, 29, 2886–2892, <https://doi.org/10.1111/gcb.16678>, 2023.
- Humphrey, V., Zscheischler, J., Ciais, P., Gudmundsson, L., Sitch, S., and Seneviratne, S. I.: Sensitivity of atmospheric CO<sub>2</sub> growth rate to observed changes in terrestrial water storage, *Nature*, 560, 628, <https://doi.org/10.1038/s41586-018-0424-4>, 2018.
- Jain, V. K., Pandey, R. P., Jain, M. K., and Byun, H. R.: Comparison of drought indices for appraisal of drought characteristics in the Ken River Basin, *Weather Clim. Ext.*, 8, 1–11, <https://doi.org/10.1016/j.wace.2015.05.002>, 2015.
- Klein Tank, A. M. G., Wijngaard, J. B., Können, G. P., Böhm, R., Demarée, G., Gocheva, A., Míleta, M., Pashiardis, S., Hejkrlik, L., Kern-Hansen, C., Heino, R., Bessemoulin, P., Müller-Westermeier, G., Tzanakou, M., Szalai, S., Pálsdóttir, T., Fitzgerald, D., Rubin, S., Capaldo, M., and Petrovic, P.: Daily dataset of 20th-century surface air temperature and precipitation series for the European Climate Assessment, *Int. J. Climatol.*, 22, 1441–1453, <https://doi.org/10.1002/joc.773>, 2002.
- Klein, T.: The variability of stomatal sensitivity to leaf water potential across tree species indicates a continuum between isohydric and anisohydric behaviours, *Funct. Ecol.*, 28, 1313–1320, <https://doi.org/10.1111/1365-2435.12289>, 2014.
- Lal, P., Shekhar, A., Gharun, M., and Das, N. N.: Spatiotemporal evolution of global long-term patterns of soil moisture, *Sci. Total Environ.*, 867, 161470, <https://doi.org/10.1016/j.scitotenv.2023.161470>, 2023.
- Lal, P., Singh, G., Das, N. N., Colliander, A., and Entekhabi, D.: Assessment of ERA5-land volumetric soil water layer product using in situ and SMAP soil moisture observations, *Geosci. Rem. Sens. Lett. IEEE*, 19, 1–5, <https://doi.org/10.1109/LGRS.2022.3223985>, 2022.
- Li, X., Xiao, J., He, B., Arain, M. A., Beringer, J., Desai, A. R., Emmel, C., Hollinger, D. Y., Krasnova, A., Mammarella, I., Noe, S. M., Ortiz, P. S., Rey-Sanchez, C., Rocha, A. V., and Varlagin, A.: Solar-induced chlorophyll fluorescence is strongly correlated with terrestrial photosynthesis for a wide variety of biomes: first global analysis based on OCO-2 and flux tower observations, *Glob. Change Biol.*, 24, 3990–4008, 2018.
- Li, X., and Xiao, J.: A global, 0.05-degree product of solar-induced chlorophyll fluorescence derived from OCO-2, MODIS, and reanalysis data, *Remote Sens.*, 11, 517, <https://doi.org/10.3390/rs11050517>, 2019.
- Li, X., Xiao, J., Kimball, J. S., Reichle, R. H., and Frankenberg, C.: Synergistic use of SMAP and OCO-2 data in assessing the responses of ecosystem productivity to the 2018 U.S. drought, *Remote Sens. Environ.*, 251, 112062, <https://doi.org/10.1016/j.rse.2020.112062>, 2020.
- Li, F., Xiao, J., Chen, J., Ballantyne, A., Jin, K., Li, B., Abrahama, M., and John, R.: Global water use efficiency saturation due to increased vapor pressure deficit, *Science*, 381, 672–677, <https://doi.org/10.1126/science.adf5041>, 2023.
- Magney, T. S., Frankenberg, C., Sun, Y., Joiner, J., Porcar-Castell, A., and Baker, I.: Mechanistic evidence for tracking the seasonality of photosynthesis with solar-induced fluorescence, *P. Natl Acad. Sci. USA*, 116, 11640–11645, 2019.
- Marchin, R. M., Backes, D., Ossola, A., Leishman, M. R., Tjoelker, M. G., and Ellsworth, D. S.: Extreme heat increases stomatal conductance and drought-induced mortality risk in vulnerable plant species, *Glob. Change Biol.*, 28, 1133–1146, <https://doi.org/10.1111/gcb.15976>, 2022.
- Markonis, Y., Kumar, R., Hanel, M., Rakovec, O., Mára, P., and AghaKouchak, A.: The rise of compound warm-season droughts in Europe, *Sci. Adv.*, 7, eabb9668, <https://doi.org/10.1126/sciadv.abb9668>, 2021.
- McDowell, N. G., Allen, C. D., Anderson-Teixeira, K., Aukema, B. H., Bond-Lamberty, B., Chini, L., Clark, J. S., Crowther, T., Frey, S., and HilleRisLambers, J.: Pervasive shifts in forest dynamics in a changing world, *Science*, 368, 1–12, 2020.
- Mishra, A. K. and Singh, V. P.: Drought modeling – A review, *J. Hydrol.*, 403, 157–175, <https://doi.org/10.1016/j.jhydrol.2011.03.049>, 2011.
- Müller, L. M. and Bahn, M.: Drought legacies and ecosystem responses to subsequent drought, *Glob. Change Biol.*, 28, 5086–5103, <https://doi.org/10.1111/gcb.16270>, 2022.
- Muñoz-Sabater, J., Dutra, E., Agustí-Panareda, A., Albergel, C., Arduini, G., Balsamo, G., Boussetta, S., Choulga, M., Harrigan, S., Hersbach, H., Martens, B., Miralles, D. G., Piles, M., Rodríguez-Fernández, N. J., Zsoter, E., Buontempo, C., and Thépaut, J. N.: ERA5-Land: A state-of-the-art global reanalysis dataset for land applications, *Earth Syst. Sci. Data*, 13, 4349–4383, <https://doi.org/10.5194/essd-13-4349-2021>, 2021.
- Peters, W., van der Velde, I. R., van Schaik, E., Miller, J. B., and Ciais, P.: Increased water-use efficiency and reduced CO<sub>2</sub> uptake by plants during droughts at a continental scale, *Nat. Geosci.*, 11, 744–748, <https://doi.org/10.1038/s41561-018-0212-7>, 2018.
- Peters, R. L., Steppe, K., Pappas, C., Zweifel, R., Babst, F., Dietrich, L., von Arx, G., Poyatos, R., Fonti, M., Fonti, P., Grossiord, C., Gharun, M., Buchmann, N., Steger, D. N., and Kahmen,

- A.: Daytime stomatal regulation in mature temperate trees prioritizes stem rehydration at night, *New Phytol.*, 239, 533–546, <https://doi.org/10.1111/nph.18964>, 2023.
- Pickering, M., Cescatti, A., and Duveiller, G.: Sun-induced fluorescence as a proxy for primary productivity across vegetation types and climates, *Biogeosciences*, 19, 4833–4864, <https://doi.org/10.5194/bg-19-4833-2022>, 2022.
- Oren, R., Sperry, J. S., Katul, G. G., Pataki, D. E., Ewers, B. E., Phillips, N., and Schäfer, K. V. R.: Survey and synthesis of intra- and interspecific variation in stomatal sensitivity to vapour pressure deficit, *Plant Cell Environ.*, 22, 1515–1526, <https://doi.org/10.1046/j.1365-3040.1999.00513.x>, 1999.
- Röthlisberger, M. and Papritz, L.: Quantifying the physical processes leading to atmospheric hot extremes at a global scale, *Nat. Geosci.*, 16, 210–216, <https://doi.org/10.1038/s41561-023-01126-1>, 2023.
- Seidl, R., Thom, D., Kautz, M., Martin-Benito, D., Peltoniemi, M., Vacchiano, G., Wild, J., Ascoli, D., Petr, M., Honkaniemi, J., Lexer, M. J., Trotsiuk, V., Mairota, P., Svoboda, M., Fabrika, M., Nagel, T. A., and Reyer, C. P. O.: Forest disturbances under climate change, *Nat. Clim. Change*, 7, 395–402, <https://doi.org/10.1038/nclimate3303>, 2017.
- Seneviratne, S. I., Zhang, X., Adnan, M., Badi, W., Dereczynski, C., Di Luca, A., Ghosh, S., Iskandar, I., Kossin, J., Lewis, S., Otto, F., Pinto, I., Satoh, M., Vicente-Serrano, S. M., Wehner, M., and Zhou, B.: Weather and Climate Extreme Events in a Changing Climate, in: *Climate Change 2021: The Physical Science Basis, Contribution of Working Group I to the Sixth Assessment Report of the Intergovernmental Panel on Climate Change*, edited by: Masson-Delmotte, V., Zhai, P., Pirani, A., Connors, S. L., Péan, C., Berger, S., Caud, N., Chen, Y., Goldfarb, L., Gomis, M. I., Huang, M., Leitzell, K., Lonnoy, E., Matthews, J. B. R., Maycock, T. K., Waterfield, T., Yelekçi, O., Yu, R., and Zhou, B., Cambridge University Press, Cambridge, United Kingdom and New York, NY, USA, 1513–1766, <https://doi.org/10.1017/9781009157896.013>, 2021.
- Shekhar, A., Buchmann, N., and Gharun, M.: How well do recently reconstructed solar-induced fluorescence datasets model gross primary productivity?, *Remote Sens. Environ.*, 283, 113282, <https://doi.org/10.1016/j.rse.2022.113282>, 2022.
- Shekhar, A., Hörtnagl, L., Buchmann, N., and Gharun, M.: Long-term changes in forest response to extreme atmospheric dryness, *Glob. Change Biol.*, 29, 5379–5396, <https://doi.org/10.1111/gcb.16846>, 2023.
- Shekhar, A., Buchmann, N., Humphrey, V., and Gharun, M.: More than three-fold increase in compound soil and air dryness across Europe by the end of 21st century, *Weather Clim. Extrem.*, 44, 100666, <https://doi.org/10.1016/j.wace.2024.100666>, 2024a.
- Shekhar, A., Hörtnagl, L., Paul-Limoges, E., Etzold, S., Zweifel, R., Buchmann, N., and Gharun, M.: Contrasting impact of extreme soil and atmospheric dryness on the functioning of trees and forests, *Sci. Total Environ.*, 916, 169931, <https://doi.org/10.1016/j.scitotenv.2024.169931>, 2024b.
- Tripathy, K. P. and Mishra, A. K.: How unusual is the 2022 European compound drought and heatwave event?, *Geophys. Res. Lett.*, 50, e2023GL105453, <https://doi.org/10.1029/2023GL105453>, 2023.
- Tsakiris, G. and Vangelis, H.: Establishing a drought index incorporating evapotranspiration, *Eur. Water*, 9/10, 3–11, 2005.
- van der Woude, A. M., Peters, W., Joetjzer, E., Lafont, S., Koren, G., Ciais, P., Ramonet, M., Xu, Y., Bastos, A., Botía, S., Sitch, S., de Kok, R., Kneuer, T., Kubistin, D., Jacotot, A., Loubet, B., Herig-Coimbra, P.-H., Loustau, D., and Luijkx, I. T.: Temperature extremes of 2022 reduced carbon uptake by forests in Europe, *Nat. Commun.*, 14, 6218, <https://doi.org/10.1038/s41467-023-41851-0>, 2023.
- van der Molen, M. K., Dolman, A. J., Ciais, P., Eglin, T., Gobron, N., Law, B. E., Meir, P., Peters, W., Phillips, O. L., Reichstein, M., Chen, T., Dekker, S. C., Doubkova, M., Friedl, M. A., Jung, M., van den Hurk, B. J. J. M., de Jeu, R. A. M., Kruijt, B., Ohta, T., Rebel, K. T., Plummer, S., Seneviratne, S. I., Sitch, S., Teuling, A. J., van der Werf, G. R., and Wang, G.: Drought and ecosystem carbon cycling, *Agr. Forest Meteorol.*, 151, 765–773, <https://doi.org/10.1016/j.agrformet.2011.01.018>, 2011.
- Zhang, J., Xiao, J., Tong, X., Zhang, J., Meng, P., Li, J., Liu, P., and Yu, P.: NIR<sub>v</sub> and SIF better estimate phenology than NDVI and EVI: Effects of spring and autumn phenology on ecosystem production of planted forests, *Agr. Forest Meteorol.*, 315, 108819, <https://doi.org/10.1016/j.agrformet.2022.108819>, 2022.
- Zhou, S., Yu, B., and Zhang, Y.: Global concurrent climate extremes exacerbated by anthropogenic climate change, *Sci. Adv.*, 9, eabo1638, <https://doi.org/10.1126/sciadv.abo1638>, 2023.
- Wable, P. S., Jha, M. K., and Shekhar, A.: Comparison of drought indices in a semi-arid river basin of India, *Water Resour. Manag.*, 33, 75–102, <https://doi.org/10.1007/s11269-018-2089-z>, 2019.
- Wang, B., Chen, T., Xu, G., Wu, G., and Liu, G.: Management can mitigate drought legacy effects on the growth of a moisture-sensitive conifer tree species, *Forest Ecol. Manag.*, 544, 121196, <https://doi.org/10.1016/j.foreco.2023.121196>, 2023.